A comparison of P5, Cuk and class E2 converters for WPT in EV battery charging

A Comparison of P5, Cuk and Class E^2 Converters for WPT in EV Battery Charging

Iman Okasili[1], Ahmad Elkhateb[1*], and Timothy Littler[1]

[1] School of Electronics, Electrical Engineering and Computer Science (EEECS), Queen's University, Belfast BT9 5AH, United Kingdom

[*]a.elkhateb@qub.ac.uk

Keywords: Inductive power transfer, Battery chargers, Compensation, E^2 Converters, Dynamic Systems.

Abstract

This paper presents three DC-DC converter topologies, P5, Cuk and a class E^2 converter to compare their performance in the context of wireless power transfer for electric vehicle battery charging. The comparisons use MATLAB simulation to explore the abilities of the system to produce the desired outputs, efficiency, and ability to operate under changing load and coupling factor conditions. The paper highlights current issues with resonant DC-DC converters for wireless electric vehicle battery charging. It also serves to draw parallels between the new application of Cuk and P5 converters for WPT, and that of the Class E^2 topology which is better understood within the context of wireless power transfer. The promising feature of Buck-Boost DC-DC converters for wireless power transfer is the ability to control output voltage from the duty cycle. This controllability opens new avenues for creating robust systems under varying coupling factors and loads. The Buck-Boost converter-based systems also benefit from a reduction in overall converters needed and a lower operating frequency than that of Class E^2 converters.

1 Introduction

Wireless power transfer (WPT) presents a means of tackling issues that traditionally have stunted the commercial success of electric vehicles (EVs). Problems with range and charging times have hindered EVs since their conception. To combat this, a significant amount of research has been conducted into battery technology and the efficiency of vehicles. However, with growing environmental concerns, increasing battery size could detract from the eco-friendly prerogative to switch to EVs. WPT not only offers a means of safe charging in various weather conditions [1] but also easy and convenient charging for users. Dynamic charging has been shown to significantly increase vehicle range with a reduction in battery size [2]. Since the conception of modern WPT for EV charging systems in the early 1990's, the overall topology of power converters has stayed the same. A typical WPT system can have up to six converter stages. On the primary side there is a rectifier to gain a DC waveform from the mains supply, there then may be up to two DC-DC converters for power factor correction and setting appropriate voltage. Following this, an inverter is used to generate the waveform needed for the transfer of power wirelessly. On the secondary there is another rectifier to regain the DC waveform for battery charging and in some cases a DC-DC converter to maintain appropriate voltage for the battery and for possible impedance matching purposes. For comparison a standard plug-in EV (PEV) may need as little as two converter stages, one rectifier to gain a DC waveform from the mains and one DC-DC converter to set appropriate voltage levels for battery charging. Converter size and complexity has been an issue studied by several over the years. Most converters employ several switches throughout their design. These switches have their own associated losses in the form of switching and conduction losses. Switching losses occur at the initial moment of switching when either the switch is opening or closing and both current and voltage are present across the switch causing a power loss. Modern converters typically require switching frequencies at kHz and above, meaning these losses can be substantial. There are two means of minimizing the loses from the switches, these are to reduce the number of switches and/or modify the power waveforms. The Class E inverter introduced in 1975 [3] is the first instance in which researchers began reducing converter size. A standard H-bridge inverter uses up to four switch to output a sinewave whereas the class E variant needs only one. Soon after the invention of the class E inverter came the class E rectifier [4] **.** The use of both the class E inverter and rectifier combination is what is now known as the class E^2 converter seen in Fig 1. Where WPT for EVs is concerned, class E^2 converters offer a means of substantially reducing converter size thus saving space and cost.

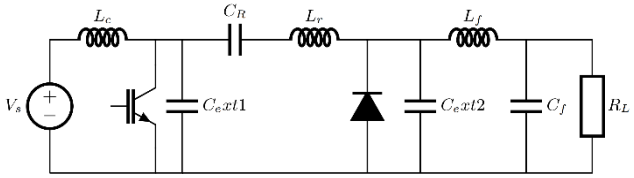

Fig. 1. Resonant Class E^2 Converter, where C_{ext1} and C_{ext2} are the associated capacitances of the switching MOSFET and diode, respectively.

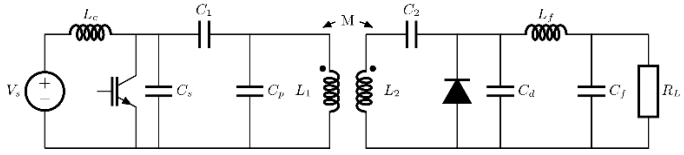

Fig. 2. Inductively Coupled Class E^2 Converter.

In recent years class E^2 converters designed as WPT systems for EV battery charging have seen an increase in attention [5]–[8]. Class E inverters can be designed to operate with zero voltage switching (ZVS), zero current switching (ZCS) and zero derivative switching (ZDS) over a range of coupling

factors and loads [9]. ZVS/ZCS is achieved by leaving a small reactance in the system to delay the voltage/current waveform when switching occurs. This minimises the time in which voltage and current are present across the initial switching moment thus minimizing power losses. ZVS/ZCS is often achieved in two ways, one is to design around a static operating frequency and include extra reactance in the system [8][10][11] or the operating frequency can be controlled to be above or below the resonant frequency to achieve the same effect [12]. For resonant converters ZVS is preferred [13]. The work in [8] showcases a design procedure for a class E^2 converter at low coupling coefficients (k < 10%). This design procedure is focused on using first harmonic analysis (FHA) of the current waveform to calculate suitable component values for the converter. In [14] it is stated that if the input current/voltage of the class E rectifier is considered as purely sinusoidal then that rectifier can be replaced by the input impedance, thus allowing it to be viewed as an AC load. To achieve ZVS there is an optimal load condition of $0 < R < R_{iopt}$, this must be considered when designing the system and the input resistance must be within this range.

Within the last 5 years a new candidate for reduced converter design in WPT systems has emerged. The work in [15] shows new isolated converter topologies for single switched Buck-Boost converters. The paper describes how the standard procedure has been to use a high frequency transformer or a pair of coupled inductors in place of one of the existing circuit inductors. The proposed method in this paper is to split the power transferring capacitor C_p and place the high-frequency transformer in between the two new capacitances C_1 and C_2 as seen in Fig. 3. Where $C_1 = C_2 = C_P$.

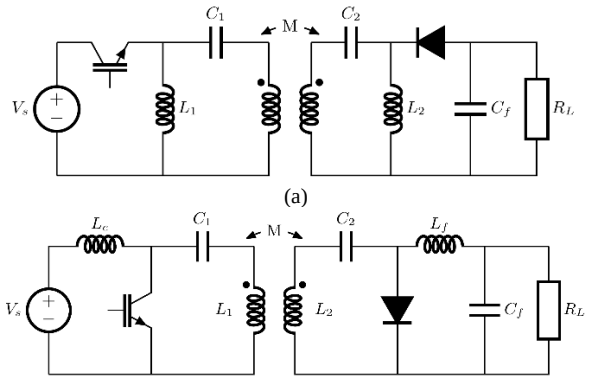

Fig. 3. WPT DC-DC Converters (a) P5 & (b) Cuk.

This allows for better utilization of the core. The paper states that when using the conventional method, magnetic energy is temporarily stored in the circuit core, thus the magnetic energy transfer is limited by core volume $\frac{1}{2} * B * H * Volume$. It then goes onto prepose that core volume is utilized more effectively if the magnetic energy is transferred is through instantaneous transformer action rather than intermediate magnetic energy storage. Multi-switch topologies such as those using full, or half bridge rectifiers utilize the core better. They achieve this through maintaining a balanced operation by alternating equally through the B-H magnetic quadrants. This balanced operation can be seen in more traditional WPT circuits that use full or half wave rectifiers in conjunction with a resonant circuit to output a sine wave for optimized power transfer. The work in [15] also showcases a new P5 topology, this topology benefits from a reduction in the size of the split capacitors plus no DC bias on the primary or secondary side.

The first instance of preposing these isolated DC-DC converter topologies for WPT EV charging can be seen in [16]. Where the Cuk, SEPIC, Zeta and P5 converter topologies are compared. The work in [16] also compares the inverting section of the Cuk converter to that of a standard H-bridge inverter. It is seen that at a duty cycle of 50% it is possible to generate a sinusoidal waveform in the inverter section of the isolated Cuk converter. The research also shows a similar efficiency curve over a range of input currents between the isolated Cuk converter and H-bridge.

2 Converter Design

a. Class E^2 Converter Design

The design methodology for the class E^2 converter is well documented in [8], [13] and [14]. The design practises explained in these works, focus on separate design of both the class E inverter and rectifier, the two separate parts are then cascaded. The fundamental reason for designing in this manner is due to when the output of the class E inverter is a pure sinusoid then any load on the inverter can be treated as a standard AC load. The design process focuses on phase angles of inverter output voltage and currents in relation to one another and the driving signals switch. In [8] there is also a preposed addition of a power transfer controlling capacitor also named C_p.

b. P5 and Cuk Converter Design

Both P5 and Cuk converters are variants of Buck-Boost converters. Designing a Buck-Boost converter to suit the power requirements of a WPT EV battery charging system needs an understanding of design from base principles. The function of the Buck-Boost converter is to convert a DC reference voltage to a new desired DC voltage across the load. A Buck-Boost converter allows for the output voltage to be greater or lower than the reference voltage it is supplied with, the total output power of the converter is the same as that it is supplied with when ignoring losses. The device that transfers energy from input to output is the capacitor C_p, this capacitor utilizes current from the input and output inductors L_1 and L_2. The current in these inductors is highly dependent on the duty cycle δ of the switch. The duty cycle is defined by the ratio between the switches On and OFF state. For steady state operation the average voltage across inductors L_1 and L_2 is zero, the average voltage across C_1 is:

$$V_{C1} = V_i - (-V_o) = V_i + V_o \quad (1)$$

Where V_i and V_o are the input and output voltages of the system respectively. When the switch is ON over the period ($\delta \rightarrow \delta T_s$) the diode is OFF and the current in C_1 is:

$$i_{Cp} = -i_{L2} \quad (2)$$

When the switch is OFF over the period ($\delta T_s \rightarrow T_s$) the diode is ON and the current in C_1 is:

$$i_{Cp} = + i_{L1} \quad (3)$$

The average capacitor current is zero, therefore:

$$- i_{L2}\delta T_s + i_{L1}(1-\delta)T_s = 0 \quad (4)$$

$$\frac{i_{L1}}{i_{L2}} = \frac{\delta}{(1-\delta)} \quad (5)$$

As mentioned, the power absorbed by the load is equivalent to the power supplied by the source:

$$\frac{V_o}{V_i} = \frac{i_{L1}}{i_{L2}} = \frac{\delta}{(1-\delta)} \quad (6)$$

From (6) it shown that the duty cycle is the main tuning parameter to consider when designing a system for a specific output.

The choosing of component values is directly linked to the needed duty cycle, due to the ripple current in a DC-DC converter playing a significant role in steady state operation. DC-DC converters can operate in two conductions modes which are continuous (CCM) and discontinuous (DCM). In almost all cases the desired conduction mode is CCM, this is due to DCM operation causing intermittent power supply to the load. To ensure that CCM is maintained component values must be chosen so that any ripple current present does not cause DCM. A relationship between inductor ripple current and the inductor value can be extrapolated from $V_L = L\frac{di}{dt}$. Whist the switch is ON:

$$V_{L1} = V_i = L_1\frac{di_{L1}}{dt} \quad (7)$$

$$\Delta i_{L1} = \frac{\partial V_i}{L_1 f_s} \quad (8)$$

And similarly, for L_2:

$$V_{L2} = V_{Cp} - V_o = V_i + V_o - V_o = V_i \quad (9)$$

$$V_i = L_2\frac{di_{L2}}{dt} \quad (10)$$

$$\Delta i_{L2} = \frac{\partial V_i}{L_2 f_s} \quad (11)$$

So, the maximum and minimum current for the inductors is:

$$i_{L1}{}_{min}^{max} = i_{L1} \pm \frac{1}{2}\Delta i_{L1} \quad (12)$$

$$i_{L2}{}_{min}^{max} = i_{L2} \pm \frac{1}{2}\Delta i_{L2} \quad (13)$$

For CCM the minimum current must be maintained above 0:

$$i_{L1} - \frac{1}{2}\Delta i_{L1} > 0 \quad (14)$$

$$i_{L1} > \frac{1}{2}\Delta i_{L1} \quad (15)$$

Due to the average current in capacitor C_2 being 0 it can be stated that $I_{L2} = \frac{V_0}{R}$, thus from (8) it can be shown:

$$i_{L1} = \frac{\delta}{(1-\delta)}\frac{V_0}{R} \quad (16)$$

By substituting (8) and (16) into (15) and rearranging for L_1 the desired range of values can be found for L_1 so that CCM is maintained:

$$L_1 > \frac{(1-\delta)^2 R}{2\delta f_s} \quad (17)$$

The same can be applied to L_2:

$$i_{L2} - \frac{1}{2}\Delta i_{L2} > 0 \quad (18)$$

$$i_{L2} > \frac{1}{2}\Delta i_{L2} \quad (19)$$

Again, by expressing the current in L_2 as $I_{L2} = \frac{V_0}{R}$ and substituting (11) into (19) the range of values for L_2 to maintain CCM is derived:

$$L_2 > \frac{(1-\delta)R}{2f_s} \quad (20)$$

The ripple voltage at the capacitors also needs to be considered to achieve good power quality. By using the AC voltage equation for a capacitor, it can be shown that:

$$\Delta V_{Cp} = \frac{1}{C_1}\int_{\delta T_s}^{T_s} i_{L1} dt \quad (21)$$

$$\Delta V_{Cp} = \frac{i_{L1}(1-\delta)T_s}{C_1} \quad (22)$$

By substituting (16) into (22) the voltage change in C_1 can be expressed as:

$$\Delta V_{Cp} = \frac{\delta V_o}{RC_p f_s} \quad (23)$$

As for C_2 it is in parallel with the load, so the AC component of current flows through the capacitor whilst the DC current passes through the load. The variation in capacitor voltage can be calculated from the relationship between capacitor voltage and current.

$$i_{c_f} = i_l - i_R \quad (24)$$

$$Q = C_f V_o \quad (25)$$

$$\Delta V_o = \frac{\Delta Q}{C_f} \quad (26)$$

The change in charge is calculated from half cycle of the current ripple:

$$\Delta Q = \frac{1}{2}\frac{T_s}{2}\frac{\Delta i_{L2}}{2} \quad (27)$$

$$\Delta Q = \frac{T_s \Delta i_{L2}}{8} \quad (28)$$

To focus on the output voltage equation (6) can be rearranged to make V_o the subject, by subbing this into equation (11) the current ripple in the inductor can be stated as:

$$\Delta i_L = \frac{V_o(1-\delta)}{Lf_s} \quad (29)$$

By substituting (29) into (28):

$$\Delta Q = \frac{V_o(1-\delta)}{8Lf_s^2} \quad (30)$$

By rearranging (26) so that ΔV_o is the subject and substituting this into (30) and dividing by V_o the voltage ripple in C_2 can be expressed as:

$$\frac{\Delta V_o}{V_o} = \frac{V_o(1-\delta)}{8LC_f f_s^2} \quad (31)$$

To transfer power wirelessly a set of coils is needed, to calculate an appropriate inductance of these coils the information in section I can be applied. From Fig. 3 the system splits the power transferring capacitance into two separate capacitances on both the transmitting and receiving side of the system. To increase the power transfer capability the system the coils will be chosen as to resonate with the split capacitance:

$$f = \frac{1}{2\pi\sqrt{LC}} \quad (32)$$

3. Simulation

In this case the system is to transfer 3kW of power, in line with the lower end of level 2 charging. A typical EU charger is supplied with 220V from the mains supply and a standard EV battery needs 400V for charging. WPT for EV charging presents a unique situation in contrast to other WPT systems for battery charging such as for phones. When charging an EV through WPT there is a significantly increased air gap to consider. To charge an EV the coils must be able to send power at distances of 200m+. The work in [17] showcases a bipolar pad design that can transfer power over 200mm with coupling factors maintained in the region of 18% ~ 32% over critical to optimal points of misalignment. For the simulation and coupling facto dependent design steps, the coupling factors within this range will be used.

a. Parameters and Components Values for Class E^2 Converter

These component values were obtained using the design method detailed in [8]. This method was chosen as it is one of the most detailed examples of resonant converter design for inductively coupled systems that operate with a low coupling factor. It should be noted that the switching frequency for this converter is 1MHz. A coupling factor of 18% was chosen as it represents a worse case scenario, it is also due to the limited range in appropriate coupling factors for design consideration for this method. The coil inductances and resistances are kept the same as in [8]. The components values seen in Table 1 were used in the simulations.

Table 1: Class E^2 Component Values

Component	Value
L_c	0.187 mH
L_f	0.262 mH
C_1	1.39 nF
C_2	1.43 nF
C_s	1.08 nF
C_p	2.53 pF
C_d	1.28 nF
C_f	9.67 nF
R_L	50 Ω

b. Parameters and Component Values for P5 and Cuk Converters

According to the guidelines set out by the SAE frequencies between *79kHz – 90kHz* [18] are selected for wireless EV charging. This system will therefore run at 80kHz. The ripple current in both inductors is chosen to be 10% whilst the voltage ripple in C_p and C_f are chosen as 5% and 1% respectively. Using the equations detailed in the design section of this paper, the values for each component can be seen in Table 2**.**

Table 2: Cuk & P5 Component Values

Component	Value
L_1	1.5 mH
L_2	2.5 mH
C_p	1.83 μF
C_f	292 nF
R_L	53.3 Ω
L_{coil}	2.02μH
Coil Resistance	0.5 Ω

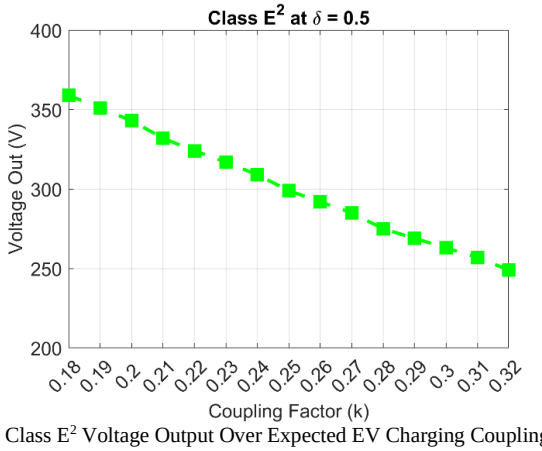

Fig. 4. Class E^2 Voltage Output Over Expected EV Charging Coupling Factor Range.

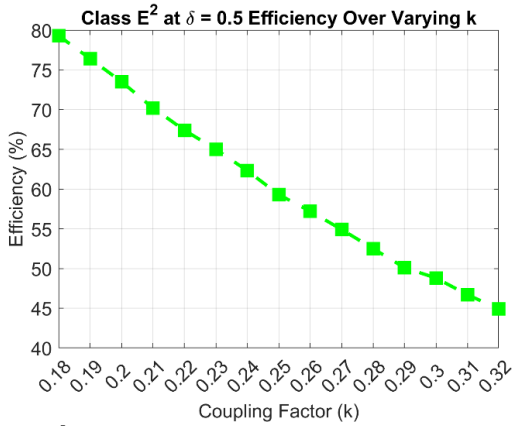

Fig. 5. Class E^2 Efficiency Over Expected EV Charging Coupling Factor Range.

c. Class E^2 Simulation Results

Figs. 4 & 5 depict the voltage and efficiency of the class E^2 converter over an increasing coupling factor. As coupling factor increases there is steady decline in both voltage output and efficiency as coupling factor increase. The problems of declining voltage and declining efficiency arise from two separate issues when applying class E^2 to WPT for EV battery charging. The voltage issue can be attributed to the relatively

high coupling factor used for these simulations. The design procedure in [8] uses a coupling factor of 5.59% which is

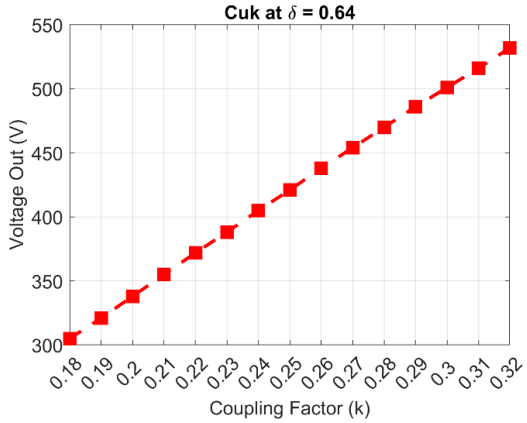

Fig. 6. Cuk Voltage Output Over Expected EV Charging Coupling Factor Range.

nearly 3 times less than the coupling factor used for design in these simulations. The higher coupling factor results in a voltage offset where the 'core' is not fully utilized, energy is being stored in the coils and transferred via intermediate inductance. The energy storage in the coils results in a higher rms voltage across the coils for a 18% coupled system than at one coupled at 5.59%. This results in a lower overall voltage seen at the output. The matter of efficiency however is to do with the change in system parameters over time. The design process used in [8] shows that several component values are reliant on a set coupling factor to maintain resonant operation. As seen from Fig. 5 when operating at the coupling factor chosen for design, the efficiency of the system is high. As coupling factor increases the resonances within the system stray and the voltage waveform is distorted causing significant losses. It can be noted that the current waveform maintains almost a perfect sinusoidal shape throughout this coupling factor variation. It should also be noted that the system exhibited both voltage and current output ripples of ~3% throughout.

d. Cuk & P5 Simulation Results

It was observed for both Cuk and P5 converters that the design method used yielded a means to achieve suitable output voltage, current and power levels. But the overall efficiency of either system rarely reached above 8% and was recorded at as little as 1%. Increasing coupling factor, changing load and/or varying duty cycle did not have a significant impact on producing a highly efficient system. The issue of efficiency in this case is once again in relation to the 'core'. This is highlighted in [15] where it is stated that a core with infinite magnetizing inductance such as that of a standard ferrite core transformer is needed for the split-capacitor waveforms of a Buck-Boost convert to utilize transformer action. In the case of coupled inductors, the magnetizing inductance is equivalent to the mutual inductance which is even less than the sum of the coupled inductance. Due to this, there is a large amount of power stored in the coils as the falling edge of the switching signal causes large voltage spikes. This in turn creates a large current draw from the power supply meaning the primary side of the system stores a large amount of power which is not transferred to the secondary side of the system. Yet, as previously mentioned the system is still able to produce desired outputs in simulations.

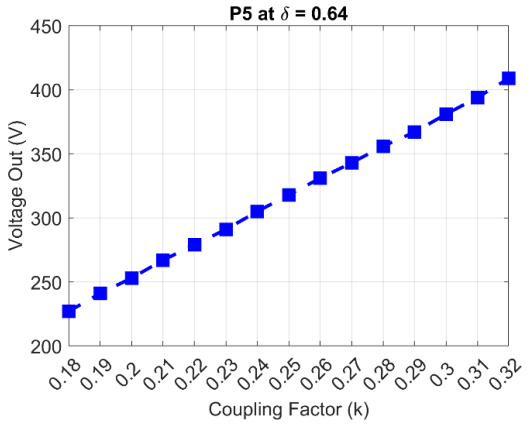

Fig. 7. P5 Voltage Output Over Expected EV Charging Coupling Factor Range.

From Figs. 6 & 7 both the Cuk and P5 topologies have their own respective specific coupling factors in which they output the desired voltages for what would have been the appropriate duty cycle. In comparison the Cuk converter maintains a higher output than that of the P5 on average over the coupling factor range and achieves the desired output at a lower coupling factor than that of the P5 topology.

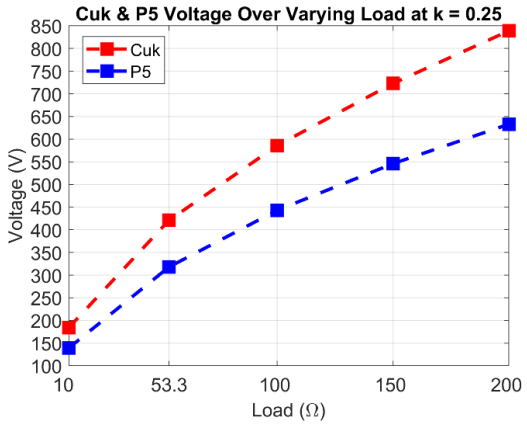

Fig. 8. Cuk & P5 Voltage Output Over Varying Load.

Fig. 8 shows the associated voltages levels over different loads. Whilst the voltages increase it was seen that neither system had a significant increase in output power, the output current had in inverse relationship with increasing load and the associated power crept from 3.3kW to 3.52kW over the entire range of the loads for Cuk. For P5 the power output showed an even smaller increase of only 0.05kW, starting at 1.95kW and reaching 2kW.

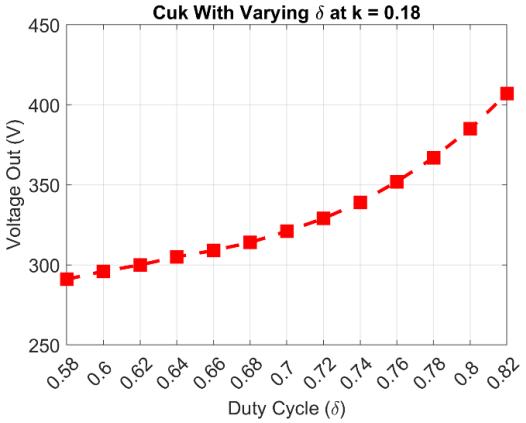

Fig. 9. Cuk Voltage Output for a Coupling factor of 0.18, Over Varying Duty Cycle.

Fig. 9 shows that a Cuk topology can reach the desired voltage output from the minimum expected coupling factor utilizing duty cycle control. In contrast the P5 system was able to approach the desired output, but the system needed a duty cycle of >95% to achieve this.

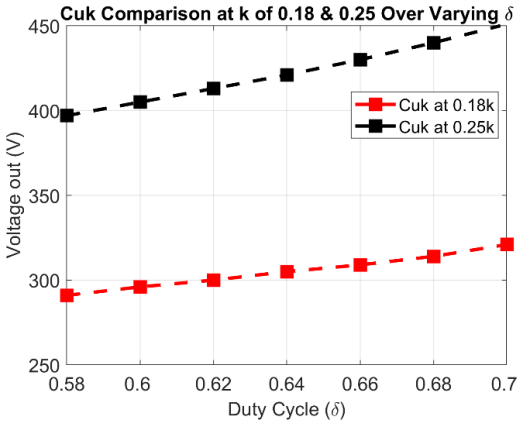

Fig. 10. Cuk Voltage Outputs for Different Coupling Factors Over Varying Duty Cycle.

Fig. 10 shows the comparison of duty cycle control at two coupling factors for the Cuk topology. This highlights the subtle difference in duty cycle sensitivity over different coupling factors. Over a 12% duty cycle increase the total voltage increase at k = 0.18 was 30V. Whereas the increase in voltage for the same duty cycle range when the system was operating at k = 0.25 was 54V. Within the same range of duty cycles at the same coupling factors the P5 controller showed little sensitivity and displayed a 1-2V increase per 2% duty cycle increase. However, the system was able to achieve the desired output at k = 0.25 with a duty cycle of 83%.

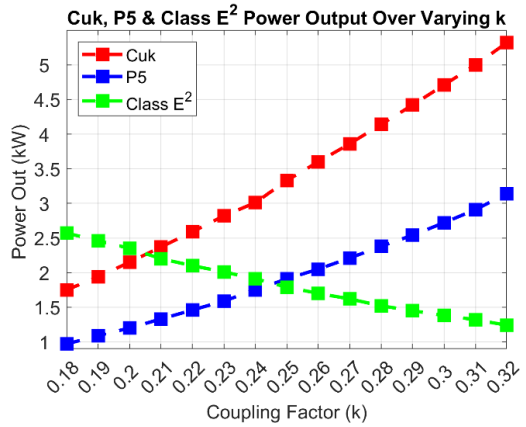

Fig. 11. Class E^2, Cuk & P5 Power Outputs Over Expected k Range.

Fig. 11 shows the power outputs over the expected coupling factor range. Both Cuk and P5 were operating with a 64% duty cycle whilst the Class E^2 converter utilized a 50% duty cycle. Using this information in tandem with previous simulations when operating at an optimum coupling factor, each system can output the desired 400V at 3kW. The most flexible of the systems is the converter which has an optimum operation point that resides almost in the centre of the expect coupling factor range. Simulations where also conducted to see if Cuk topology was able to operate during the more extreme circumstances. It was found that the Cuk topology was able to utilize duty cycle control to achieve a desire output voltage at all coupling factor ranges.

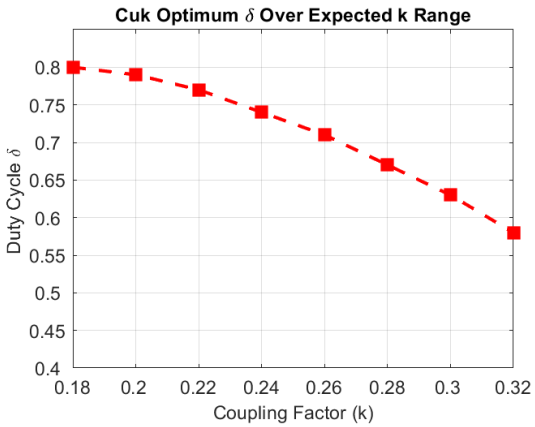

Fig. 12. Cuk Optimum Duty Cycle for Corresponding Coupling Factors.

Fig. 12 shows the matching duty cycle needed to achieve the desired output over the expect coupling range. Simulation showed that at the matching duty cycle the system was consistently able to output the desired 400V at 3kW. The voltages and power outputs seen are within 1% and 3% tolerances of their respective desired outputs. Through duty cycle control it is possible to maintain the appropriate voltage on the output even in the case of a 200Ω load at a coupling factor of 32%. This output was achieved at a duty cycle of 21%. However, in this case the power output dropped to 0.79kW.

Table 3. Cuk Outputs with different Coil Quality/Coupling Factors

Cuk Outputs at k = 0.18			
Coil Quality Factor	Voltage Out (V)	Current Out (A)	Power Out (kW)
Q = 2	305	5.73	1.75
Q = 10	781	14.63	14.4
Cuk Outputs at k = 0.25			
Quality Factor	Voltage Out (V)	Current Out (A)	Power Out (kW)
Q = 2	421	7.91	3.33
Q = 10	979	18.35	16.9
Cuk Outputs at k = 0.32			
Quality Factor	Voltage Out (V)	Current Out (A)	Power Out (kW)
Q = 2	532	10	5.32
Q = 10	1140	21.36	24.3

$$Q = \frac{\omega L}{R} \quad (33)$$

Equation 36 was used to calculate the quality factor for the coils in the system. Where $\omega = 2 * \pi * frequency$ and L and R are the inductance and resistance of the coil respectively. Since both the sending and receiving coils are of the same inductance, their resistance has been kept the same mean the quality factors shown in Table 3 correspond to both the sending and receiving coil. Table 3 shows that the system is highly sensitive to quality factor, these quality factors were used to represent the general lower and upper limits in which coils this size would display. The quality factor had an impact on a few key aspects of the system which are the output current, output voltage and the overall system efficiency. In some cases, with a higher quality factor the efficiency was over 16%. It was also seen that changing the quality factor did not affect the systems ability avail of duty cycle control.

4 Discussion

From the simulation results the Class E^2 converter exhibited the ability to efficiently transfer power to a charging EV. However as coupling factor increases the efficiency of the system lowers. This may not be a major issue as achieving lower coupling factors is an easier hill to surmount than producing a system with higher coupling factors. However, the design process for WPT Class E^2 is one that focuses on a stagnant or predetermine coupling factor. This is not the case in EV charging as parking position and height of vehicle from the charging pad mean that there may be different coupling factors in each use case. The Class E^2 converter needs at least one Buck-Boost converter to supply it with appropriate voltage levels to charge the EV battery from a typical mains supply. This increases the total number of converter stages needed which in turn increases system size, cost, complexity, and losses. A resonant Buck-Boost converter will streamline the overall system which should allow for increased adoption at lower costs. From the simulations and research detailed in this paper it is evident that resonant Buck-Boost topologies have the capability to deliver and control the power needed to charge an EV. From the two leading candidates, the Cuk topology seems to be the more robust option. The Cuk topology displayed the ability to deliver the desired voltage over the entire expected range of coupling factors and loads. The Cuk topology was also able, in most cases, to maintain the desired power level. Although the Cuk topology did fail to maintain the desired power level when the both the coupling factor and load were entering their upper limits. The Cuk topology entered a steady state operation within 30ms. Changing the duty cycle during simulation showed that when increasing the duty cycle, the output initially drops and then moves towards the new target output. The inverse was seen when lowering the duty cycle.

5 Conclusion

The research conducted in this paper serves to showcase and prove the ability of a resonant Buck-Boost topology to wirelessly deliver desired voltage and power to a charging EV load. However, some major issues exist with the current technology. These issues stem from the sharp voltage and current changes due to the switch. In systems with a full H-bridge circuit these issues are not present, as sinusoidal current and voltage waveforms are seen in the transmitting coil. By further studying the resonant Buck-Boost system and improving on its design it may be possible to replicate the sinusoidal waveform seen in the coils of the Class E^2 converter. Future research will be aimed at re-evaluating the split capacitor design procedure and implementing the voltage shaping capacitors seen in the Class E^2 converter. This would seem to be possible as comparing the Cuk topology to the Class E^2 converter, it is apparent that they are very similar. The desired outcome will be to gain a sinusoidal voltage waveform across the coils with lower input current whilst also maintaining the ability to control output parameters with duty cycle control. The aim of this research is to produce a heavily streamlined and highly controllable WPT system as current systems for EV charging can be space consuming and costly.

6 Acknowledgement

I. Okasili would like to acknowledge the PhD scholarship provided by the Department for Economy (DfE), Northern Ireland, to carry out this research.

This work was supported in part by the UK Engineering and Physical Sciences Research Council (EPSRC) under Grant EP/T026162/1. For the purpose of open access, the author has applied a Creative Commons Attribution (CC BY) licence to any Author Accepted Manuscript version arising.

References

[1] N. H. Kutkut and K. W. Klontz, "Design considerations for power converters supplying the SAE J-1773 electric vehicle inductive coupler," in *Conference Proceedings - IEEE Applied Power Electronics Conference and Exposition - APEC*, 1997, vol. 2, pp. 841–847.

[2] N. P. Suh, D. H. Cho, and C. T. Rim, "Design of on-line electric vehicle (OLEV)," in *Global Product Development - Proceedings of the 20th CIRP Design Conference*, 2011, pp. 3–8.

[3] N. O. Sokal and A. D. Sokal, "Class E-A New Class of High-Efficiency Tuned Single-Ended Switching Power Amplifiers," *IEEE Journal of Solid-State Circuits*, vol. 10, no. 3, pp. 168–176, 1975.

[4] R. J. Gutmann, "Application of RF Circuit Design Principles to Distributed Power Converters," *IEEE Trans. Industrial Electronics and Control Instrumentation*, vol. IECI-27, no. 3, pp. 156–164, 1980.

[5] W. X. Chen and Q. H. Chen, "Application of class-E converter in magnetic resonant WPT system," in *AUS 2016 - 2016 IEEE/CSAA International Conference on Aircraft Utility Systems*, Nov. 2016, pp. 320–324.

[6] T. Nagashima, K. Inoue, X. Wei, E. Bou, E. Alarcon, and H. Sekiya, "Inductively coupled wireless power transfer with class-E2 DC-DC converter," 2013.

[7] T. Nagashima, X. Wei, E. Bou, E. Alarcón, M. K. Kazimierczuk, and H. Sekiya, "Steady-State Analysis of Isolated Class-E2 Converter Outside Nominal Operation," *IEEE Trans. Industrial Electronics*, vol. 64, no. 4, pp. 3227–3238, Apr. 2017.

[8] T. Nagashima, X. Wei, E. Bou, E. Alarcon, M. K. Kazimierczuk, and H. Sekiya, "Analysis and design of loosely inductive coupled wireless power transfer system based on class-E2 DC-DC converter for efficiency enhancement," *IEEE Trans. Circuits and Systems I: Regular Papers*, vol. 62, no. 11, pp. 2781–2791, Nov. 2015.

[9] A. Ayachit, F. Corti, A. Reatti, and M. K. Kazimierczuk, "Zero-voltage switching operation of transformer class-E inverter at any coupling coefficient," *IEEE Trans. Industrial Electronics*, vol. 66, no. 3, pp. 1809–1819, Mar. 2019.

[10] C. Liu, S. Ge, Y. Guo, H. Li, and G. Cai, "Double-lcl resonant compensation network for electric vehicles wireless power transfer: Experimental study and analysis," *IET Power Electronics*, vol. 9, no. 11, pp. 2262–2270, Sep. 2016.

[11] S. Li, W. Li, J. Deng, D. Nguyen, and C. C. Mi, "A Double-Sided LCC Compensation Network and Its Tuning Method for Wireless Power Transfer," *IEEE Trans. Vehicular Technology*, vol. 64, no. 6, 2015.
[12] A. Babaki, S. Vaez-Zadeh, A. Zakerian, and G. A. Covic, "Variable-Frequency Retuned WPT System for Power Transfer and Efficiency Improvement in Dynamic EV Charging with Fixed Voltage Characteristic," *IEEE Trans. Energy Conversion*, 2021.
[13] M. K. Kazimierczuk and J. Jwik, "Resonant dc/dc Converter with Class-E Inverter and Class-E Rectifier," *IEEE Transactions on Industrial Electronics*, vol. 36, no. 4, pp. 468–478, 1989.
[14] M. K. Kazimierczuk and D. Czarkowski, *Resonant Power Converters*, 2nd ed. Wiley, 2011.
[15] B. W. Williams, "Transformer Isolated Buck-Boost Converters," 2016. http://apc.aast.edu/ojs/index.php/RESD/article/viewFile/02.2.112/89 (accessed Mar. 16, 2021).
[16] A. Elkhateb, G. Adam, and D. J. Morrow, "DC-to-DC Converter Topologies for Wireless Power Transfer in Electric Vehicles," in *IECON Proceedings*, Oct. 2019, vol. 2019-Octob, pp. 1665–1669.
[17] T. D. Nguyen, S. Li, W. Li, and C. C. Mi, "Feasibility study on bipolar pads for efficient wireless power chargers," in *Conference Proceedings - IEEE Applied Power Electronics Conference and Exposition - APEC*, 2014, pp. 1676–1682.
[18] "J2954: Wireless Power Transfer for Light-Duty Plug-in/Electric Vehicles and Alignment Methodology - SAE International." https://www.sae.org/standards/content/j2954_202010/ (accessed Mar. 12, 2021).